nature communications

Article

https://doi.org/10.1038/s41467-024-54307-w

Biomass competition connects individual and community scaling patterns

Received: 25 March 2024

Accepted: 6 November 2024

Published online: 15 November 2024

Check for updates

Lorenzo Fant [1,2] & Giulia Ghedini [1,3]

Both metabolism and growth scale sublinearly with body mass across species. Ecosystems show the same sublinear scaling between production and total biomass, but ecological theory cannot reconcile the existence of these nearly identical scalings at different levels of biological organization. We attempt to solve this paradox using marine phytoplankton, connecting individual and ecosystem scalings across three orders of magnitude in body size and biomass. We find that competitive interactions determined by biomass slow metabolism in a consistent fashion across species of different sizes. These effects dominate over species-specific peculiarities, explaining why community composition does not affect respiration and production patterns. The sublinear scaling of ecosystem production thus emerges from this metabolic density-dependence that operates across species, independently of the equilibrium state or resource regime. Our findings demonstrate the connection between individual and ecosystem scalings, unifying aspects of physiology and ecology to explain why growth patterns are so strikingly similar across scales.

Ecosystems show remarkable regularities that suggest that their functioning is bound by common organising principles[1–4]. One of these regularities is the sublinear scaling between biomass production and total biomass, which follows a power law (often near ¾) that is independent of the ecosystem considered[3]. Different ecosystems thus grow at similar rates mainly determined by their total biomass, independently of species size and composition. These size-independent patterns are at odds with the sublinear scaling of metabolism with size observed for individual organisms, and their origin remains unclear[3,5,6]. Recent work shows that the sublinear scaling of ecosystem production can emerge if populations of different species themselves grow sublinearly[7]. However, the apparent incompatibility between ecosystem-level and individual-level scalings remains unresolved[7–9].

Why are the two scalings incompatible? Across most taxa, individual metabolism and growth scale sublinearly with body mass following a power law with an exponent $\beta < 1$[6,10,11] (Fig. 1a). This sublinear scaling implies that, while larger organisms have greater metabolic (or growth) rates in an absolute sense, they consume less energy per unit mass compared to smaller organisms (valid for any scaling $\beta < 1$). Therefore, the size of organisms should affect the functioning of populations and communities. Two systems (populations or communities) of equal biomass density but different size composition should not have the same metabolism or growth: a system composed of smaller organisms should respire/grow faster than a system of larger organisms if $\beta < 1$ (and the other way around if $\beta > 1$). Since ecosystem metabolism and production increase with total biomass at a similar rate ($\alpha \sim ¾$)[1,3], the metabolic theory of ecology would predict that this pattern results from changes in species size[12]: ecosystems of larger biomass should be dominated by larger organisms that have lower metabolism per unit mass[5]. However, empirical data do not support this explanation as size structure is nearly invariant across ecosystems (or does not change sufficiently to explain this ecosystem pattern)[3,5]. An alternative hypothesis is that sublinear scaling in ecosystems is a consequence of density-dependent processes that slow production as biomass accumulates[3,7,8,13]. But how these processes operate to control biomass growth in such a consistent way across species and ecosystems – positing a common underlying mechanism – remains unknown.

We attempt to solve this puzzle by overcoming a limitation of the metabolic theory of ecology. It is often assumed that metabolism-size relationships of organisms in isolation hold for these same organisms in communities, but this assumption has little empirical support[13–16]. Competition for resources alters energy use, and many species reduce

[1]Instituto Gulbenkian de Ciência (IGC), Oeiras, Portugal. [2]Istituto Nazionale di Oceanografia e di Geofisica Sperimentale (OGS), Trieste, Italy. [3]Gulbenkian Institute for Molecular Medicine (GIMM), Oeiras, Portugal. e-mail: lorenzofant@gmail.com; giulia.ghedini1@gmail.com

https://doi.org/10.1038/s41467-024-54307-w

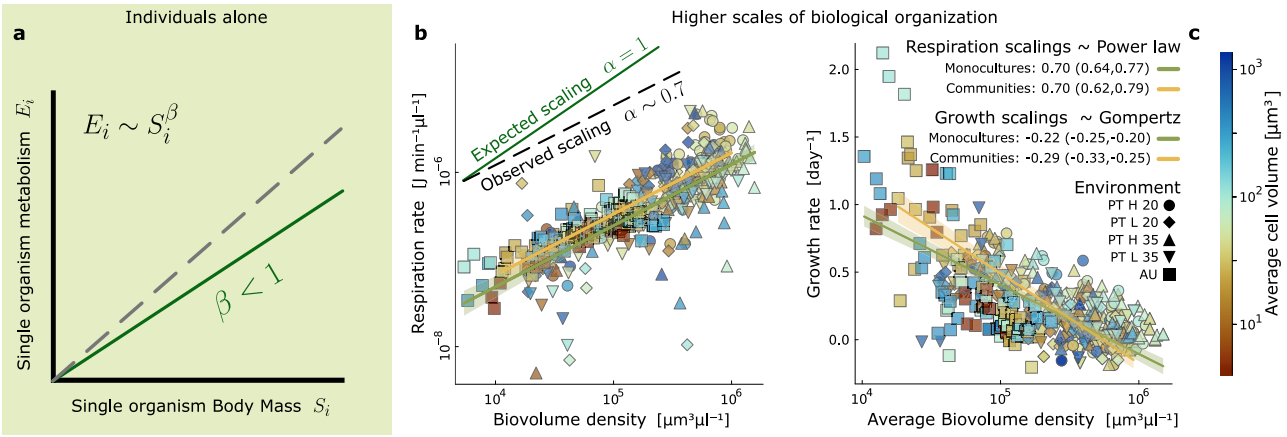

Fig. 1 | Respiration and growth scale sublinearly with total biovolume across monocultures and communities with no effect of species size. a The respiration and growth of individual organisms scale sublinearly ($\beta < 1$) with body size across most taxa: $E_i \sim S_i^{\beta}$. **b** This sublinear scaling at the individual level should affect the respiration and growth of monocultures and communities. In particular, total metabolism should increase linearly with total biomass for all monocultures since they are composed of organisms of similar size: $E \sim \sum_i^N S_i^{\beta} \sim N\bar{S}^{\beta} = B\bar{S}^{\beta-1}$ (expected scaling ~ B) because the total number of organisms $N = B/\bar{S}$. Instead, total respiration (**b**) and growth (**c**) scale sublinearly with biovolume even if species size varies by three orders of magnitude. Note that growth is analysed against the geometric mean of biovolume ln-transformed but plotted on a $\log_{10}$ scale for consistency. Lines (**b**, **c**) represent the fit value from the model and 95% confidence interval. Symbols refer to the geographic location (AU = Australia, PT = Portugal), light (High vs Low) and salinity (35 vs 20 ppt). Source data are provided as a Source Data file.

their respiration rate in denser populations[17–23]. We provide a formal account of how these density-dependent processes affect organismal metabolism, biomass production, and their scaling with body size. We explore both metabolism and growth because, while they are correlated, it is unclear which one drives the other[24]. By doing so, we demonstrate that the effect of competition on organismal metabolism is the key to reconciling individual and ecosystem scalings.

We base our assessment on marine phytoplankton, a system of global importance for primary production[25,26]. The size diversity of this system allows us to explore scaling relationships across three orders of magnitude in body size[27] at different scales (individuals, populations, species pairs, communities), measuring metabolism as both respiration and photosynthesis. To demonstrate the generality of our findings we use geographically separate and independent phytoplankton communities (Australia, AU[20] and Portugal, PT), and measure them under a total of five environmental conditions in the laboratory. In each location, we source five species from local culture collections and grow them alone (monocultures) or together (communities). In the first location (AU), we also test all pairs of species and grow all cultures under ideal conditions of light (115 µmol photons m^{-2} s^{-1}) and salinity (35 ppt). In the second location (PT), we grow cultures under four combinations of light (High vs Low, corresponding to 60 and 30 µmol photons m^{-2} s^{-1}, respectively) and salinity (35 vs 20 ppt), creating a range of suboptimal environments. We start all cultures from a small biovolume of phytoplankton (a proxy for biomass, obtained as the product of cell volume and cell number); we then track changes in cell size, biovolume density, growth, and metabolism (photosynthesis, respiration) from exponential to stationary phase. These data allow us to evaluate the effects of individual size on community functioning and quantify the effect of biomass competition on metabolism across growth phases and environments.

Results

Organismal size does not affect metabolism and growth at higher scales of organisation

Organismal respiration scales sublinearly with size across species, including phytoplankton[26]. Therefore, we would predict that species of different sizes (or communities with different size structures) should function at different rates. The effect of size should be particularly obvious for monocultures since all phytoplankton cells in a population have a similar size: total population respiration should scale linearly with total biovolume and with a size-dependent slope (intercept on a log-log scale, Fig. 1a, b).

Contrary to this prediction, we find that phytoplankton cell size does not influence total respiration rates even if species vary in size by three orders of magnitude ($F_{1,\ 95} = 0.77$; $p = 0.38$). Instead, total respiration scales sublinearly with total biovolume across monocultures and communities (α ~ 0.70, obtained by fitting a power law; Fig. 1b), with values that are consistent with those observed in terrestrial and aquatic ecosystems[1,3]. Similarly, we find no effect of species size on total growth rate ($F_{1,\ 518} = 1.21$; $p = 0.27$), which declines with increasing biovolume with slopes ~ − 0.25 (− 0.22 for monocultures and − 0.29 for communities, calculated by fitting a Gompertz curve; Fig. 1c). Cell size also does not influence the sublinear scaling of total photosynthesis with biovolume ($F_{1,91} = 0.42$, $p = 0.52$; Supplementary Fig. 1a).

Importantly, we do not wish to provide a specific scaling exponent that is valid for all systems because the environment affects these relationships[28]. Geographic location, level of organisation and environmental conditions affected both intercepts and scaling exponents (see Supplementary Note 1, Supplementary Figs. 1–3 and Supplementary Tables 1–3). However, cell size does not explain this variability. Even when accounting for both differences between species and environments, scaling exponents and intercepts do not correlate with cell size (Supplementary Fig. 4 and Supplementary Table 5). So, while the environment affects scaling patterns and we cannot exclude species-specific differences, total biovolume (not individual size) appears the primary driver of population/community metabolism and growth (Fig. 1 and Supplementary Fig. 5).

Our simplified phytoplankton system, therefore, shows the same incompatibility between individual- and community-level scalings observed for other systems[3,13,28–30]. These two sublinear scalings seem incompatible because community metabolism (or growth) can be independent of species size only if individual metabolism scales isometrically (not sublinearly) with body size[13].

Resolving the paradox: the coexistence of sublinear and isometric scaling at the individual level

Here, we demonstrate, first mathematically and then empirically, that sublinear and isometric scaling at the individual level can coexist

because they pertain to different comparisons: traditional comparisons across species, which focus on intrinsic species traits, i.e., differences in body size (that yield sublinear scaling, $\beta < 1$), and comparisons of interacting individuals embedded in an environment with the same biomass density (that yield an isometric scaling, $\beta = 1$). We base our reasoning on respiration, but we demonstrate below that the same holds for growth and photosynthesis. We define the scaling exponent at the individual level with β to distinguish it from the scaling exponent α of populations or communities as in Fig. 1.

As observed in Fig. 1, total metabolism scales with total biomass as $E \sim B^{\alpha}$ independently of the average size $\bar{S}$ of organisms[1,3,13] (see also Supplementary Fig. 4). If we consider systems at a fixed biomass density B^*, the number of organisms N is inversely proportional to their average size $\bar{S}$ so that $B^* = N\bar{S}$[31]. Given that the average metabolism $\bar{E}_i$ of organisms in a population or community is equivalent to the total metabolism E divided by the number of individuals N, we inevitably find a linear relationship between individual size and metabolic rate:

$$\bar{E}_i = \frac{E}{N} \sim \frac{(B^*)^{\alpha}}{B^*/\bar{S}} = (B^*)^{\alpha-1}\bar{S} \propto \bar{S} \quad (1)$$

Since biovolume is fixed, B^* is a constant. The result of Eq. 1 is independent of the scaling exponent observed between total metabolism E and total biomass B (the value of α). Community metabolic scaling could follow any trend, but as long as it is not affected by size composition, it still leads to an isometric scaling between individual metabolism and size at a fixed biomass density (Fig. 2a), and vice versa.

If we instead consider systems at fixed population densities (number of organisms $N = N^*$, including traditional estimates of individual metabolic scaling based on $N^* = 1$), the average size of organisms becomes just a proxy for total biomass. Thus, when evaluating the individual metabolic rate as a function of its size, one retrieves the initial scaling of metabolism to biovolume observed in communities (Supplementary Fig. 6):

$$\bar{E}_i = \frac{E}{N^*} \sim \frac{B^{\alpha}}{N^*} = \frac{(N^*)^{\alpha}\bar{S}^{\alpha}}{N^*} = (N^*)^{\alpha-1}\bar{S}^{\alpha} \propto \bar{S}^{\alpha} \quad (2)$$

If we could quantify the scaling α at progressively lower N^*, until $N = 1$, then we would directly connect the scaling exponent β of individual organisms to the exponent α of populations/communities.

If neither biomass nor the number of organisms is fixed, metabolism can scale with size in several ways (Supplementary Fig. 6). Since metabolism-size relationships are often estimated for different organisms in varying conditions of population or biomass density, this variability could partly explain the inconsistencies in scaling exponents reported in the literature[6,10,32], including for phytoplankton[26,33].

Therefore, if the observation of Fig. 1 is correct (i.e., total metabolism scales with biomass independently of organismal size), competition with an equal amount of biomass shifts the scaling of individual metabolism with body size from sublinear (Eq. 2) to isometric (Eq. 1).

We validate these theoretical predictions with empirical data by testing the scaling between individual metabolic and production rates with cell size at a fixed biomass density. We use the full range of biovolumes of our system by rescaling all data points to a single biovolume value in the centre of the range (10^5 µm^3 µl^{-1}; Supplementary Fig. 7 for rescaling approach). As predicted, both organismal metabolism and production scale isometrically (linearly) with cell size at a fixed biovolume in monocultures (Fig. 2b respiration and production,

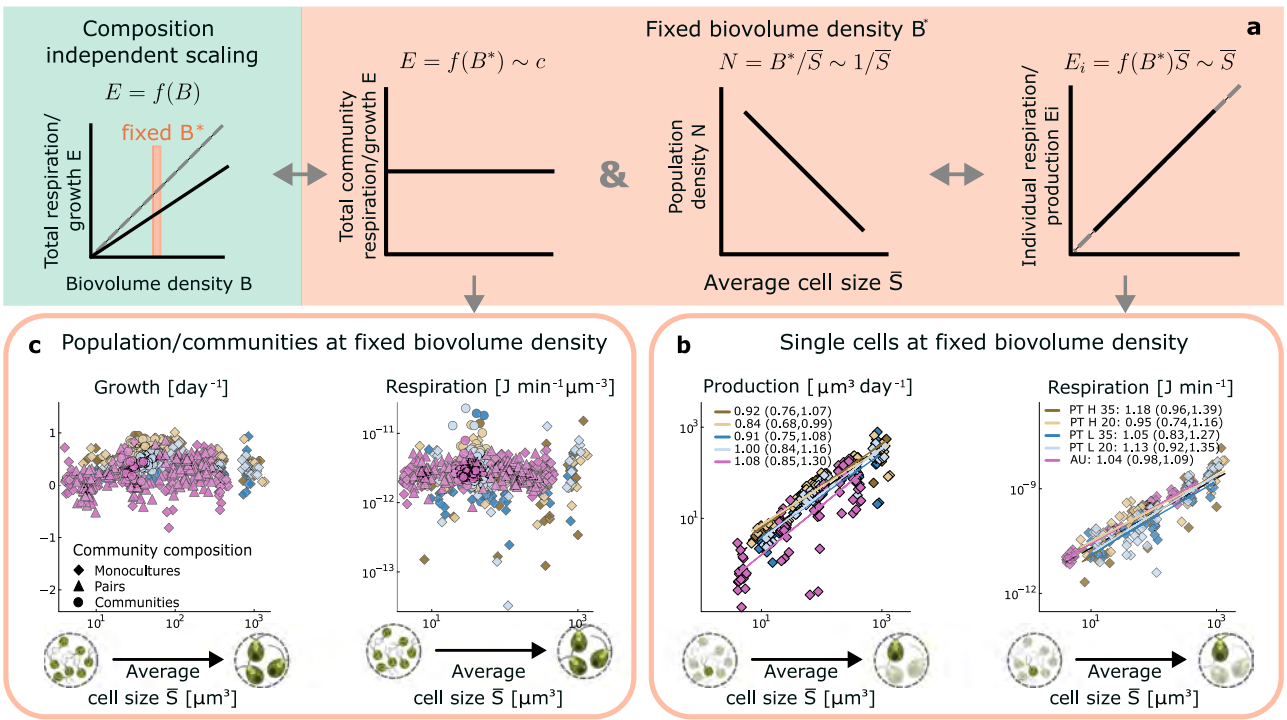

Fig. 2 | Theoretical predictions and empirical validation of the isometric scaling between individual metabolism and size in systems at fixed biomass density. **a** If species size does not affect the scaling between total metabolism and total biomass density (as observed in Fig. 1), individual metabolism should scale isometrically with size in systems at fixed biomass density B^*. The same should hold for production (biomass growth). **b** We confirm this result empirically: individual respiration (J/min per cell) and production rates (µm^3/day) scale linearly with cell size across phytoplankton species and environments when comparing organisms at the same biovolume density (10^5 µm^3 µl^{-1}). Here, we only use data from monocultures, but the scaling is robust even when considering data from communities (Supplementary Fig. 9). **c** As a consequence of isometric scaling, organismal size has no effect on the total respiration or growth rates of systems at the same biovolume density. Whole population/community rates are divided by total biovolume (thus are J min^{-1} µm^{-3}). Colours identify the treatment based on geographic location (AU = Australia, PT = Portugal), light (High vs Low) and salinity (35 vs 20 ppt). Source data are provided as a Source Data file.

Supplementary Fig. 8d photosynthesis). This result also holds for the *per capita* metabolic rates of "average" individuals in mixtures of species (pairs and communities; Supplementary Fig. 9) and when rates are rescaled to a range of fixed biovolumes (Supplementary Fig. 10). By demonstrating this theoretical result, we quantitatively validate our observation: community metabolism and biomass growth are independent of species composition and average size because organisms of different sizes respire and grow at the same rate per unit mass when compared at equivalent biomass densities (Fig. 2c respiration and growth, Supplementary Fig. 8a–c photosynthesis). We further show that individual metabolism and production scale sublinearly with cell size in most environments at fixed population densities (all photosynthesis and production rates scale sublinearly; the scalings of respiration are more variable and include exponents below (AU, H 35, H 20), above 1 (L 35) and close to 1 (H 20) with large confidence intervals that overlap 1 in most conditions; Supplementary Figs. 10, 11).

Notably, the variability in scaling exponents observed at fixed population densities collapses onto isometric scaling at fixed biovolume densities for all rates considered (i.e., when we compare small and large phytoplankton cells competing with the same amount of total biovolume, Fig. 2 and Supplementary Fig. 8). This shift in scaling implies that an increase in total biomass affects the metabolism of different organisms in a very similar way, independently of their size and identity, and regardless of how biovolume is distributed (i.e., many small or few large organisms, as shown in Fig. 2b). The metabolism and production of an organism are thus more tightly regulated by the total biomass with which it interacts than by its size. Since here we used data from monocultures, the total biovolume is composed only of conspecifics. If this result also holds in communities (i.e., is independent of biovolume composition), then we can explain why ecosystem production patterns show no effect of species size and composition.

Everybody is anybody: community composition does not affect metabolic density-dependence

In the previous section, we found that biomass competition affects metabolism and production in the same way across individual species (monocultures). Here we investigate whether these effects persist when species interact in communities. Specifically, we use monoculture data to predict the metabolism and growth of our phytoplankton communities, testing the importance of two factors (Fig. 3a):

1. biomass composition: does the biomass of other species (interspecifics) reduce organismal metabolism in the same way as the biomass of conspecifics?
2. species identity: how important are species-specific differences in growth and metabolism (Supplementary Fig. 3) when predicting community rates?

We start by testing the relative effects of intra- and inter-specific competitors on organismal respiration (1), assuming species identity matters (2) (as before, we base our reasoning on respiration). We use species-specific relationships between respiration and biovolume in each environment (Supplementary Table 4) to calculate the metabolism per unit biovolume of each species in the community, according to two extreme hypotheses (Fig. 3a):

a. competition for resources is stronger within species than among species[34], so only conspecifics reduce the metabolism of an organism while interspecific competitors have negligible effects; hence metabolism per unit biovolume e_s of each species s declines only in response to the biomass density of conspecifics: $e_s \sim {B_s}^{\alpha_s - 1}$.
b. phytoplankton species compete for similar resources, so intra- and inter-specific competitors have equal effects on metabolism; hence, the metabolism per unit biovolume of each species declines in response to the total biovolume density of the community: $e_s \sim {B_{tot}}^{\alpha_s - 1}$.

We estimated the respiration of each species in the community using each approach since we know the biomass density of conspecifics B_s and the total biomass of the community B_{tot} at each point in time. Finally, we calculated the total community respiration rate as the sum between species (predicted rates; see Methods for details) and compared these predictions with rates measured experimentally on communities throughout their growth.

Predictions based on the total community biovolume are accurate (hypothesis b; Fig. 3b). Conversely, if we do not account for interspecific competitors (hypothesis a), we overestimate community rates – in other words, we underestimate the level of metabolic suppression driven by competition. Thus, on average, respiration declines identically in response to intra- and inter-specific competitors. To further test this result, we explored an intermediate situation in which interspecifics might affect metabolism in a weaker way than conspecifics. To do this, we estimated the effects of each species on one another using data from pairs of species (this test was only possible for AU data). Despite its greater specificity, this approach does not improve predictions (Supplementary Figs. 12–14).

Now we challenge our second assumption: does species identity matter? We find that identity has negligible effects. If we randomise the association between species-specific declines in respiration rates and the biovolume of species in the community, we obtain a distribution of estimates that contains the prediction made before, using the correct association (Fig. 3c). So, predictions based on randomised associations perform similarly to species-specific predictions. The variability in metabolic density-dependence between species, therefore, does not meaningfully affect community predictions, at least based on our experimental accuracy. Importantly, the randomised distribution does not contain the prediction based on conspecific biovolume (hypothesis a), confirming that the biovolume of all competitors is the quantity that affects species respiration in communities.

If species identity has weak effects, then we can ignore it and estimate a general relationship between respiration and biomass by merging all species data (in each environment). So, instead of the expectation based on metabolic theory $E \sim \sum_i^N S_i^\beta$, we find

$$E \sim \sum_s^n B_s e_s \sim \sum_s^n B_s {B_{tot}}^{\alpha_s - 1} \sim {B_{tot}}^{\alpha} = \left(\sum_i^N S_i \right)^{\alpha} \quad (3)$$

where E is total respiration, $s \in [1, n]$ identifies species in a community and $i \in [1, N]$ identifies individual organisms (in populations or communities).

Despite the simplicity of this approach, based on a generalised decline in respiration with biomass across species, we can correctly predict community rates in all environments and across all growth phases (Fig. 3d). This approach ("general scaling") performs worse than that based on species-specific rates ("whole community") but is still within the randomised distribution (Fig. 3c). So we cannot state that there is no variability in metabolic responses between species, but this variation is not sufficiently strong to affect community predictions based on a species-naïve approach (see Supplementary Note 2 for details on the importance of species identity). Thus, even in a community of interacting species, respiration slows with increasing biomass at the same rate on average among species, regardless of the nature of the biomass (i.e., the relative abundance of intra- and interspecifics, and their size).

All the considerations we have done for respiration extend to biomass growth (Fig. 3d and Supplementary Fig. 15) but only partially hold for photosynthesis. Total biomass (not conspecific biomass) is still the relevant quantity to consider when predicting community photosynthesis (Supplementary Fig. 16a, as observed for respiration in Fig. 3). But species identity has stronger effects (Supplementary Fig. S16b), probably because of the unimodal scaling of photosynthesis with cell size (Supplementary Fig. 8, which is not obvious for

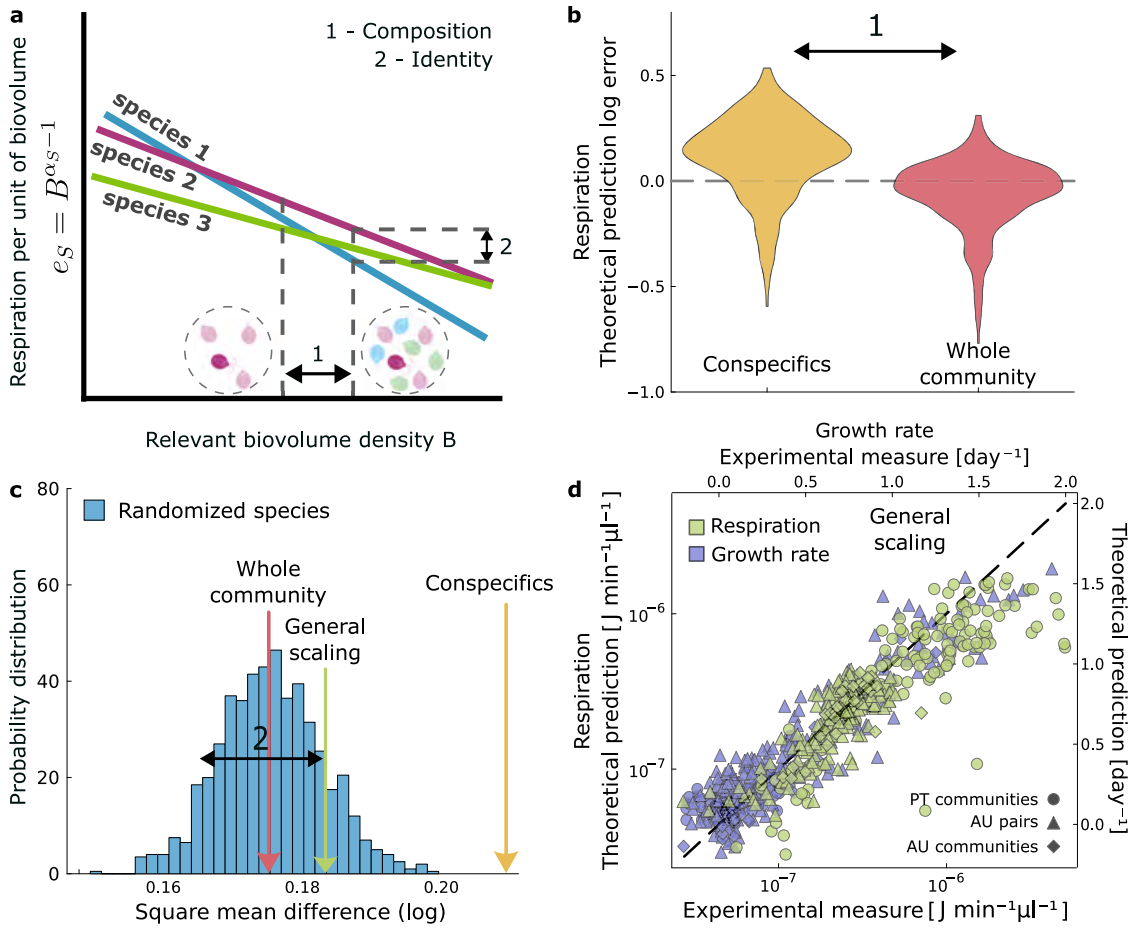

Fig. 3 | Predictions of community respiration based on different models of metabolic density-dependence. a Schematic showing species-specific declines in respiration rates per unit biovolume with increasing biovolume. We use these species-specific relationships, based on monoculture data in each environment, to test the importance of two factors on community metabolism: (1) biomass composition (are metabolic declines driven equally by intra- and inter-specific competitors?), (2) species identity (do species-specific differences considerably affect community rates?). **b** Error of the predictions testing factor 1. We can correctly estimate community respiration rates if we consider the total biovolume of the community. If we account only for conspecifics, we overestimate community rates. **c** Species identity (factor 2) does not significantly affect community respiration. If we randomise the association between species-specific declines in respiration and the biovolume of species in the community, we obtain a distribution of estimates (blue) that contains the prediction made using the correct association ("whole community", magenta). Predictions based on conspecifics are outside of this range. **d** Since species identity has minimal effects, we can estimate total community respiration (green) or growth (purple) using a general scaling between respiration (growth) per unit mass and total biomass across all species (green arrow in panel **c**, refers to respiration). Abbreviations: AU = Australia, PT = Portugal. See Supplementary Figs. 15 and 16 for growth and photosynthesis. Source data are provided as a Source Data file.

respiration and growth) and the fact that species-specific responses to light availability are more pronounced for photosynthesis than respiration (Supplementary Figs. 1, 2).

Environmental conditions highlight the link between community growth and metabolism

Community metabolism and growth slow as biomass increases independently of size composition across all the environments we considered. In this last section, we leverage differences in environmental conditions to explore the connection between these density-dependent rates. We focus on photosynthesis and growth because they both respond strongly to light availability, while this is less obvious for respiration (Supplementary Figs. 1, 2).

Light availability modifies the density-dependence of community growth and photosynthesis rates per unit biovolume, but these rates remain highly correlated within each environment (Fig. 4a, b). Furthermore, once we account for differences in light intensity (AU = 115 µmol photons m^{-2} s^{-1} > PT High = 60 > PT Low = 30), photosynthesis and growth rates converge across all environments (Fig. 4c). Both growth and photosynthesis thus respond to increases in biovolume in a very similar way, indicating a strong level of community regulation that holds across environments.

We cannot establish if photosynthesis metabolism governs growth or the other way around[24]. But our data show that biomass competition slows metabolism in a very similar and predictable fashion across species (Fig. 2) so that the density-dependent patterns observed in individual populations (Fig. 1)[18] extend to entire communities throughout their whole growth process (i.e., both when far and close to equilibrium; Fig. 4).

Discussion

Ecosystem productivity scales predictably with total biomass, independently of species size and composition[3]. These size-independent patterns seem incompatible with the sublinear scaling of growth and metabolism observed at the individual level within most taxa[5,10,26]. We demonstrate the connection between these scalings by showing that biomass competition influences organismal metabolism identically across species of different sizes that compete for similar resources. These species grow, photosynthesise and respire at different rates per unit mass when compared at equal population densities, thus focusing

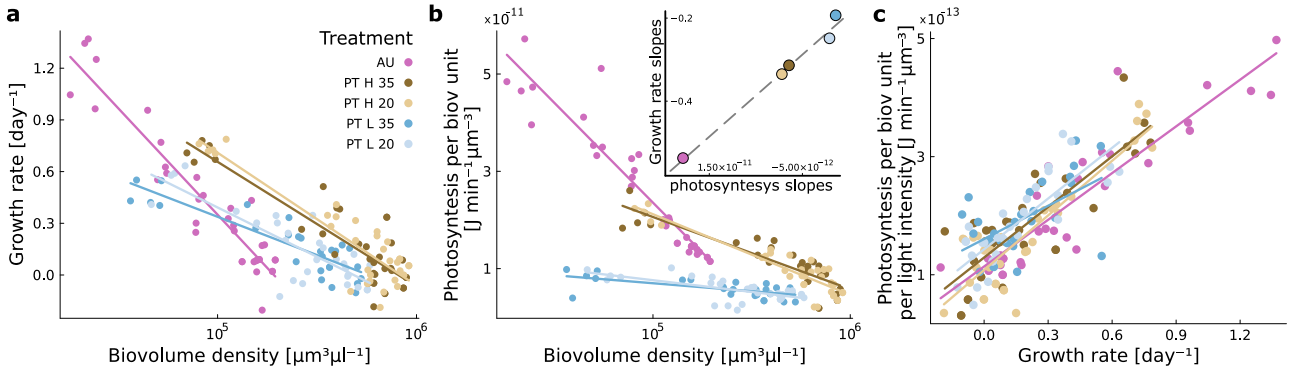

Fig. 4 | Declines in community growth rates mirror reductions in photosynthesis rates across environments. Growth (**a**) and photosynthesis rates per unit biovolume (**b**) decline with total biovolume density at different rates depending on the environment, primarily determined by light availability. All rates are calculated as the geometric mean between consecutive measurements. The insert in (**b**) shows that the rates at which growth and photosynthesis per unit biovolume decline with biomass (slopes) are highly correlated (the broken line has a slope of 1). **c** Differences in light availability explain variation in both photosynthesis and growth, as these rates converge across all environments once we standardise photosynthesis for light intensity. Colours identify the treatment based on geographic location (AU = Australia, PT = Portugal), light (High vs Low) and salinity (35 vs 20 ppt). Source data are provided as a Source Data file.

on body size properties (i.e., classic organismal metabolism-size relationships). However, the (mostly) sublinear scaling between individual metabolism or production with body size collapses onto isometric (linear) scaling when we compare species at equivalent biomass densities. Thus, competition with an equal amount of biomass alters individual scalings in a defined and predictable way that holds across species, growth phases and environments, and is independent of the composition of the biomass. This result solves some of the inconsistencies and variability in metabolic scalings[21,29,35–38] (reviewed in refs. 10,26) and shows how essential it is to account for changes in metabolism in response to competition when estimating scaling exponents.

Many species show metabolic density-dependence in response to intraspecific competition, including prokaryotes[39], unicellular[18,21] and multicellular eukaryotes[17,22]. The effects of interspecific competition on metabolism, however, have been explored in a handful of studies[13,40], so it is difficult to predict how competition between species affects community functioning. If species in a community compete for similar resources, it might not be surprising that their metabolism and growth decline with increasing (biomass) competition from other species. What is surprising is that community composition only minimally influences these metabolic declines. While our communities are less diverse than natural systems, we intentionally chose phytoplankton species from different functional groups, with different sizes (3 orders of magnitude) and pigments that are known to mediate competitive interactions[41–43]. The general effects of biomass competition seem to prevail over these species-specific traits.

One exception is for photosynthesis. Community photosynthesis was estimated more precisely from species-specific rates (rather than a species-naïve "general" approach), possibly because some of our species can obtain energy from different sources (e.g., *Amphidinium* may also function as a mixotroph[44]) or have different capacity to intake or store resources (which can be size-dependent)[30,42]. Photosynthesis rates, indeed, tend to have an unimodal distribution with cell size, which indicates that species of intermediate sizes have higher photosynthetic rates than smaller or larger phytoplankton[30]. Therefore, per capita photosynthetic rates might respond differently to increases in conspecific or heterospecific biomass, affecting community predictions. These species-specific differences were less apparent for respiration and growth.

A limitation of working with phytoplankton is that we cannot measure the metabolism of single cells in isolation ($N = 1$); we need to estimate it from a population measurement. Despite the variability in scaling exponents reported for phytoplankton, a recent review indicates that photosynthesis and respiration scale mostly sublinearly with cell size across algal phyla[26]. The per-cell scaling exponents we obtain when rescaling at the same population densities are clearly sublinear for photosynthesis and growth but are more variable for respiration. This variability might be explained by a combination of stressful environmental conditions (metabolic scaling relationships often differ between environments[28,45]) and greater experimental error on respiration rates which are lower than photosynthesis rates in an absolute sense. To explore the generality of our results, we manipulated two environmental factors (light and salinity) that are important for phytoplankton, but we cannot extrapolate how biomass competition affects metabolism-size scaling in other environments. Nonetheless, our data track the entire growth process of communities, from far to equilibrium until carrying capacity spanning different growth phases and nutrient regimes. The effects of biomass competition on individual metabolism-size relationships were consistent across all of them (Fig. 2).

Importantly our results do not mean that all species in a community are equally affected by the biomass of intra- and inter-specific competitors. To test this, we would need to measure the metabolic response of individual species in a community which is experimentally unavailable. Competition theory and research suggest that intraspecific competition is often stronger than interspecific competition[34,46], so we would expect differences in how species metabolism responds to intra- and inter-specific competitors. Our results suggest that even if there are differences in species responses, these balance each other out at the community level or are sufficiently small that they can be ignored. This result, while it also shows that populations growth sublinearly, is not compatible with the sublinear growth model presented in Hatton et al.[7]; in their model, density-dependence is given by the biomass of conspecifics only, while interspecific competitors affect growth with a different functional form which is not what we observe.

Phytoplankton species compete for similar and essential resources (light and nutrients), so this system might show a strong level of community regulation that might be weaker for species that use substitutable resources. Nonetheless, our simplified system shows similar patterns (no effect of species size on community rates) to those observed in a variety of ecosystems at or near carrying capacity[3,47], including phytoplankton communities in nature[29], mesocosms[48], or over longer successional trajectories in the laboratory[13]. This consistency suggests that species interactions, such as competition for resources, can lead to strong regulation of community functioning so that community-level patterns are more consistent than those at the

individual or population level[8]. We look forward to studies that test these ideas in organisms that compete for non-essential resources and for which metabolism can be measured individually.

In conclusion, we find that increases in total biomass lead to consistent changes in metabolism across species that are interacting in a community. We do not know the specific mechanism behind these responses, but ecosystems can display allometric patterns of resource transport efficiency similar to size-dependent patterns of organismal metabolism[1,4]. So the generalised metabolic decline we observe with biomass might emerge because of geometric factors (increases in total biomass density alter the flow of resources according to common organising principles)[1,4] and behavioural or physiological adjustments to biomass density that are similar between species[17,19,21–23,49,50]. The resulting scaling patterns might thus be independent of the specific nature of interactions, at least when species compete for similar resources[8,51]. We offer the first empirical demonstration of this hypothesis[8] and show that community functioning is tightly integrated – to the point that extending the relationship between metabolism and mass from organisms to entire communities can give a reliable representation of community functioning.

Methods

Experimental setups

We combined two geographically distinct datasets of marine phytoplankton. Both datasets used species of marine phytoplankton obtained from culture collections; species were cultured in temperature-controlled rooms at 22 ± 1 °C using autoclaved Guillard's f/2 medium, prepared with filtered natural seawater.

The first dataset (AU) is from Ghedini et al.[20], where they grew five species of marine phytoplankton in three species diversity treatments over 10 days: monoculture, pairs or communities with all five species. Each monoculture and species pair were replicated three times and communities five times ($N = 50$ cultures). The work was performed at Monash University, Australia, and the species were obtained from the Australian National Algae Culture Collection: *Amphidinium carterae* (CS-740), *Tetraselmis* sp. (CS-91), *Dunaliella tertiolecta* (CS-14), *Tisochrysis lutea* (CS-177) and *Synechococcus* sp. (CS-94). All cultures were placed in cell culture flasks filled to 100 ml and grown on a 14–10 hr light-dark cycle under non-saturating irradiance levels (115 µmol photons m^{-2} s^{-1}) at ambient salinity (35 ppt). Flasks were shaken and randomly rearranged on the shelves every day. Nutrients were added daily by replacing 10% of the medium from each flask with fresh f/2 medium. All cultures were started with an initial total biovolume ~ 6×10^8 µm^3 (~ 10^3 µm^3 µl^{-1}), where biovolume is the product of cell size (volume) and number of cells and is used as a proxy for biomass in phytoplankton. Cultures were sampled on each day for the first five days and on alternate days afterwards for a total of eight sampling times (days 0, 1, 2, 3, 4, 6, 8, 10).

The second dataset (PT, unpublished) was collected at the Instituto Gulbenkian de Ciência (previously IGC, now GIMM) in Portugal using five phytoplankton species obtained from the Roscoff Culture Collection (France): *Amphidinium carterae* (RCC88), *Dunaliella tertiolecta* (RCC6), *Phaeodactylum tricornutum* (RCC2967), *Tisochrysis lutea* (RCC90), *Nannochloropsis granulata* (RCC438). These species were grown either alone in monoculture or together in a community for 16 days under two levels of salinity (35 or 20 ppt) and light (60 or 30 µmol photons m^{-2} s^{-1}) in cross combination to simulate a gradient of stressful environments. We set up 5 replicate communities (a mix of the five species in equal biovolumes) and 2 replicate monocultures of each species for each level of salinity and light in glass bottles filled with 200 ml ($N = 60$ cultures). The position of the cultures was randomised at each sampling day and cultures were bubbled continuously for mixing. We started with an initial total biovolume of ~ 4×10^9 µm^3 (~ 10^3 µm^3 µl^{-1}) for each treatment. We tracked changes in the abundance, size, and biovolume of species over time through microscopy; concomitantly, we measured the metabolism of monocultures and communities using respirometry (photosynthesis and respiration). We maintained salinity treatments by adding small amounts of distilled water when needed. Communities and monocultures were sampled on 7 and 6 occasions, respectively, over the course of 16 days to measure changes in biovolume and metabolism as detailed below (days 2-5-7-9-13-15 for monocultures, 2-3-7-9–12-14-16 for communities).

Cell size, population and biovolume density

In both experiments, 1 ml of sample from each culture was fixed with 1% Lugol's solution to quantify cell size and abundance. From these fixed samples, we loaded 10 µl onto a cell counting chamber (Neubauer improved), and we took photos of the sample with an Olympus IX73 inverted microscope using 400x magnification. Photos were processed in Fiji/ImageJ[52] to quantify the cell volume (µm^3), number of cells of each species (µl^{-1}), and biovolume as their product (µm^3 µl^{-1}). Cell volume was calculated from the major and minor axis of each cell by assigning to each species an approximate geometric shape (prolate spheroid for all species, except *Synechococcus*, *Tisochrysis*, and *Nannochloropsis* for which we assumed a spherical shape)[53]. The total biovolume of species mixtures (pairs or communities) was calculated as the sum of each individual species' biovolume.

Metabolism

Photosynthesis and respiration rates were measured from changes in percentage oxygen saturation under light (photosynthesis) or dark conditions (respiration) using 24-channel sensor dish readers (SDR; PreSens Precision Sensing GmbH, Germany). Measurements were performed in 5 ml (AU) or 2 ml (PT) glass vials with integrated oxygen sensors approximately in the middle of the photoperiod.

The system was calibrated with 100% and 0% oxygenated water prior to each experiment. We quantified photosynthesis as the rate of oxygen production under the same light intensity at which the cultures were grown, over a period of 30 min or less if cultures approached 250% earlier (the maximum value the instrument can read). Respiration was quantified as the rate of oxygen decline over 30 min following light exposure. We added a 2% solution of sodium bicarbonate to each vial to avoid carbon limitation during photosynthesis. We added blanks prepared with the supernatant of the samples on each SDR reader to account for drift and bacterial respiration (12 and 24 each sampling day for the two datasets, respectively).

In both experiments, the rate of photosynthesis or respiration of the whole sample (VO_2; units µmol O_2/min) was measured as $VO_2 = 1 \times ((m_a m_b)/100 \times V\beta O_2)$ following[54], where m_a is the rate of change of O_2 saturation in each sample (min^{-1}), m_b is the mean O_2 saturation across all blanks (min^{-1}), V is the sample volume in litres and βO_2 is the oxygen capacity of air-saturated seawater for the temperature and salinity of the sample (µmol O_2/L). The first three minutes of measurements were discarded for all samples for photosynthesis. Respiration rates were calculated after 10 min of dark when rates showed a linear decline. Rates of photosynthesis and respiration (µmol O_2/min) were converted to calorific energy (J/min) using the conversion factor of 0.512 J/µmol O_2[55] to estimate energy production and energy consumption, respectively, as in previous work[56].

Data analysis

Data were analysed and visualised through a Julia pipeline, using linear mixed effect models in RStudio (version 4.3.1) to test for differences in exponents and intercepts.

1. Data filtering: We discard negative respiration measures. Negative values of respiration are obtained when the slope of the blanks is steeper than that of the sample, which indicates either some error in the preparation/seal of the vial or that the sample does not contain enough (live) phytoplankton biomass to differentiate their respiration from that of bacteria (blanks). The number of

discarded samples is: 12/197 (PT monocultures), 11/279 (PT communities), and none in the other dataset: 0/105 (AU monocultures), 0/210 (AU pairs), 0/35 (AU communities). Similarly, we discard negative photosynthesis values (38 in total: 24 PT monocultures, 14 PT communities). We also removed day 0 for all analyses as we did not have metabolic data on that first day.

2. Data normalisation: Respiration rates, photosynthesis rates, and total biovolume values are normalised by the sample volume (2 ml for PT data, 5 ml for AU data), so they are reported in J min^{-1} μl^{-1} or μm^3 μl^{-1} respectively.
3. Growth rate: Calculated as $g_{l,t} = \frac{\ln(B_{l,t'}/B_{l,t})}{t'-t}$. Where $B_{l,t}$ and $B_{l,t'}$ are two total biovolume measurements performed on sample l at time t and $t' > t$. For the AU experiment, we calculated growth based on 90% of the previous biovolume because, on each sampling day, we removed 10% of the sample.
4. Scaling of community/population rates to total biovolume and the effect of species size on these rates: We fit a linear relationship between the logarithm of respiration (photosynthesis) rates and the logarithm of biovolume density. Still, we do not assume that there is an intrinsic power law relationship between these two quantities. In fact, the growth in biovolume we observe for each replicate is smaller than two orders of magnitude, not allowing us to establish a reliable functional form. Nonetheless, the log-log relationship allows us to find a functional form enabling the following analysis. For all analyses below, we used linear mixed-effect models, including sample ID (code) as a random effect to account for repeated measures. Respiration, photosynthesis, and biovolume were $\log_{10}$-transformed prior to analyses. Growth was analysed untransformed using the geometric mean of biovolume (ln-transformed); this fits a Gompertz growth function which seems to fit our data better than a power law or GLV. The fits were done by grouping data in the following ways:
   a – Overall scaling of monocultures and communities (Fig. 1 and Supplementary Fig. 1a): we use total respiration (photosynthesis, growth) as response variable and the interaction between total biovolume and scale (monocultures, communities) as predictors. Species pairs are excluded from this analysis because they are present in only one environment (AU, see analysis below). We also test for the effect of species size on each rate, including average size ($\log_{10}$-transformed) as the predictor, on the combined monoculture and community data.
   b – Differences in scaling between environments (Supplementary Figs. 1, 2): we analysed the data separately for each geographic location. We used linear mixed-effect models, including the interaction between biovolume and scale (monocultures, pairs, communities) for AU data. For PT data, we used biovolume, scale (monocultures, communities) and treatment (orthogonal combinations of low/high light and 20/35ppt salinity) as predictors. Interactions were removed when $p > 0.25$.
5. Species-specific scalings: We used monoculture data to estimate the relationship between respiration (photosynthesis, growth) and total biovolume for each strain in each environment (Supplementary Fig. 3 and Supplementary Table 4). While some species are the same in the two datasets (i.e., *Amphidinium*, *Dunaliella*, *Tisochrysis*), they are different strains (genetically and geographically distinct). Thus, we consider them independently. We use the ordinary least squares method (OLS) which is recommended when the error on the x-axis (biovolume) is smaller than the error on the y-axis (metabolism) and consistent with previous work[3]. We test the effect of size on monoculture rates using average size ($\log_{10}$-transformed) and geographic location (AU, PT) as predictors (Supplementary Fig. 5 and Supplementary Table 5).
6. Rescaled individual metabolic rate at fixed biovolume or cell density: Here, we want to evaluate the slope of metabolism-size relationships when species are at the same biovolume or cell density. To do this, we use the monoculture data to rescale the respiration (photosynthesis, growth) rate of each species (at the population level) to the value predicted at a fixed biovolume. To do this, we use a species and environment-specific scaling (obtained in 5; reported in Supplementary Table 4). In this way, every datapoint k of species s was rescaled independently as $E_k^* = E_k \cdot \left(\frac{B^*}{B_k}\right)^{\alpha_{h,s}}$ where E_k is the measured respiration rate of datapoint k, B_k is the measured total biovolume, B^* is the target (fixed) biovolume density (10^5 μm^3 μl^{-1}), and $\alpha_{h,s}$ is the exponent of the power law fitted at fixed environment h and species s. Such rescaling keeps the spread of the data on the y-axis (respiration rates) intact while removing variation on the x-axis (biovolume). The same procedure can be performed to fix the cell density N^* to a value $\widetilde{E}_k^* = E_k \cdot \left(\frac{N^*}{N_k}\right)^{\alpha_{h,s}}$. We can rescale by density using the exponent of the biovolume dependence as $\frac{N^*}{N_k} = \frac{N^* \bar{S}_s}{N_k \bar{S}_s} = \frac{B_s^*}{B_{k,s}}$. We used a biovolume density of 10^5 μm^3 μl^{-1}, which was in the centre of the range for Fig. 2. Similarly, we rescaled metabolic rates to a population density of 10^4 cells μl^{-1} which was a compromise between small and large species. We used a population density of 10^3 for growth as the larger species had many negative values at 10^4. We report the values of the scaling exponents obtained for a wider range of biovolumes and population densities (relevant to our cultures) in Supplementary Fig. 10.
   Average individual respiration rate: by rescaling the total biovolume to a fixed value, we lost the information on the total number of individuals. We know both B^* and the average size of each species for each datapoint $\bar{S}_k$, thus the number of individuals is $N_k(B^*) = \frac{B^*}{\bar{S}_k}$. We thus divide the total respiration rates at fixed biovolume E_k^* by $N_k(B^*)$ to calculate individual respiration rates at each timepoint. Finally, we estimate the scaling exponent of the relationship between rescaled cell rates and cell size (Fig. 2) using linear mixed-effect models (with code as a random effect). Data were analysed separately for AU and PT data as the latter also included a size by treatment interaction (light and salinity). All rates were $\log_{10}$-transformed, including individual biovolume production.
7. Predictions of community rates from monoculture rates:
   a – Respiration and photosynthesis rates per unit of biovolume: We divide the measured respiration rates of each datapoint by the total biovolume $e_k := \frac{E_k}{B_k}$. We then fit a linear relationship between the logarithm of rates per unit of biovolume and the logarithm of biovolume density. Here we fit the data by grouping for (i) species and environment (species-specific scaling; note that these scalings are simply the ones obtained in point 5 minus one that is $\alpha_{h,s} - 1$), or (ii) environment only (general scaling).
   b – Predict community rates from monoculture data: We use the relationship between Respiration/photosynthesis rate per unit of biovolume and population biovolume density obtained for monocultures (point 7a) to predict the metabolism per unit of biovolume in each community with three methods:
   - Conspecifics: we use the fits defined in 7a-i (environment and species) to calculate the metabolic rate of biovolume for each species and in each environment from the biovolume density of conspecifics present in the community at each time point. This approach assumes that the metabolism of a species is only responsive to the presence of conspecifics, while other species have no effect. We then sum over all species to find the community total metabolism.
   - Whole community: we use the same fits above (environment and species, 7a-i) to calculate the metabolic rate of

biovolume for each species and in each environment from the total biovolume density of the community at each time point. This approach assumes that the metabolism of a species is equally affected by competitors, independently of their nature – it does not matter who your competitors are, only how much biomass density surrounds you. We then sum over all species to find community total metabolism;

- General scaling: we use a general (not species-specific) relationship between metabolism per unit of biovolume and biovolume that varies between environments; we calculate it grouping by environment only (7a-ii). This approach assumes that the metabolism of a species is affected by biovolume in a way that is species-independent. Identity does not matter; competition affects everyone in the same way.

To estimate community growth we use directly the fits obtained in point 5 (species by environment) because growth is already per unit of biovolume. The "general" scaling was calculated for growth in a similar way as above, i.e., grouping by environment only.

c – Predictions of community metabolism (respiration or photosynthesis) based on species pairs*:* We calculate the effect of intraspecific competition in species pairs by fitting the difference between the expected metabolism per unit of biovolume of each species s in each datapoint k (based on monoculture data) $e_{s,k,predicted} \sim B_{s,k}^{\alpha_{h,s}-1}$ and the average metabolism per unit of biovolume measured on pairs $e_{tot,k,measured} = \frac{E_{tot,k,measured}}{B_{tot,k,measured}}$, where $B_{tot,k} = B_{s,k,measured} + B_{p,k,measured}$ and $E_{tot,k} = E_{s,k} + E_{p,k}$ but for metabolism E we cannot know the relative contribution of species s and species p (we can only measure the total).

Specifically, we fit a linear relationship to the distribution of points with coordinates:

$$X = \log(B_{tot,k,measured}) - \log(B_{s,k,measured})$$

$$Y = \log(e_{tot,k,measured}) - \log(e_{s,k,predicted})$$

In this way, we can estimate the effect of each species on each other, obtaining the slopes $\gamma_{p,s}$ that express the effect of the species p on species s. The obtained values are used to estimate the effect of *all* interspecific competitors on the metabolism per unit biovolume of each species in a community as

$$e_{s,k,all} = e_{s,k,predicted} \cdot \prod_{p \neq s} \left(\frac{B_s + \sum_{j=1}^{p} B_j}{B_s + \sum_{j=1}^{p-1} B_j} \right)^{\gamma_{p,s}} \quad (4)$$

The total community rates are then obtained by summing the contribution of each species as $E_{k,predicted} = \sum_{s=1}^{n} e_{s,k,all} B_{s,k,measured}$.

d – Predictions of community growth rates based on species pairs*:* we calculate the effect of intraspecific competition in species pairs by fitting the difference between the expected growth of each species s in each data point k (based on monoculture data) $g_{s,k,predicted} \sim B_{s,k} \alpha_{h,s}$ and the average growth measured on pairs $g_{tot,k,measured}$ calculated as in point 3 above. Then, we fit a linear relationship to the distribution of points with coordinates:

$$X = \log(B_{tot,k,measured}) - \log(B_{s,k,measured})$$

$$Y = g_{tot,k,measured} - g_{s,k,predicted}.$$

In this way, we can estimate the effect of each species on each other, obtaining the slopes $\gamma_{p,s}$ that express the effect of the species p on species s. The obtained values are used to estimate the effect of *all* interspecific competitors on the metabolism per unit biovolume of each species in a community as

$$g_{s,k,all} = g_{s,k,predicted} + \sum_{p \neq s} \left[\ln\left(B_s + \sum_{j=1}^{p} B_j\right) - \ln\left(B_s + \sum_{j=1}^{p-1} B_j\right) \right] \quad (5)$$

The total community rates are then obtained by summing the contribution of each species as $g_{k,predicted} = \frac{\sum_s g_{s,k,all} B_{s,k,measured}}{\sum_s B_{s,k,measured}}$.

e – Prediction error*:* We calculated the difference (delta) between the estimates obtained above and the empirical measures of community rates (on a log scale for respiration and photosynthesis) to visualise the offset of the prediction for each hypothesis.

f – Randomisation: We randomised the association between biovolumes and species-specific scalings by shuffling the exponents $\alpha_{h,s}$ across species as $\alpha_{h,p(s)}$, where $p(s)$ is the reshuffling function of species s. Than predictions are made as $E_k \sim \sum_s B_{s,k} B_{tot,k}^{\alpha_{h,p(s)}-1}$ for metabolism. We used a similar approach for growth.

8. Relationship between photosynthesis and growth across environments: We calculate the geometric mean of photosynthesis rates per unit biovolume between consecutive measurements to have a quantity relatable to the average growth rate (which is also calculated between consecutive measurements, point 3). We then plot the relationship between photosynthesis per unit biovolume (geom. mean) and biovolume density, and between growth and biovolume density. Here biovolume is also the geometric mean and is $\log_{10}$-transformed in both cases. Finally, to highlight the connection between these rates and account for differences in light intensity between treatments, we normalise photosynthesis by light intensity and plot it against growth.

Reporting summary

Further information on research design is available in the Nature Portfolio Reporting Summary linked to this article.

Data availability

All data used and generated in this study have been deposited in the Figshare database under the accession code https://doi.org/10.6084/m9.figshare.25234837. The dataset previously used for reference 20 (Ghedini et al.[20] Func. Ecol.) is also accessible on Figshare at https://doi.org/10.26180/16665964. Source data are provided in this paper.

Code availability

All code used in this study is available on Figshare: https://doi.org/10.6084/m9.figshare.25234837.

References

1. Nidzieko, N. J. Allometric scaling of estuarine ecosystem metabolism. *Proc. Natl. Acad. Sci. USA* **115**, 6733–6738 (2018).
2. Perkins, D. M. et al. Consistent predator-prey biomass scaling in complex food webs. *Nat. Commun.* **13**, 4990 (2022).
3. Hatton, I. A. et al. The predator-prey power law: Biomass scaling across terrestrial and aquatic biomes. *Science* **349**, https://doi.org/10.1126/science.aac6284 (2015).
4. Garlaschelli, D., Caldarelli, G. & Pietronero, L. Universal scaling relations in food webs. *Nature* **423**, 165–168 (2003).
5. Cebrian, J. Energy flows in ecosystems. *Science* **349**, 1053–1054 (2015).
6. White, C. R., Alton, L. A., Bywater, C. L., Lombardi, E. J. & Marshall, D. J. Metabolic scaling is the product of life-history optimization. *Science* **377**, 834–839 (2022).

7. Hatton, I. A., Mazzarisi, O., Altieri, A. & Smerlak, M. Diversity begets stability: Sublinear growth and competitive coexistence across ecosystems. *Science* **383**, eadg8488 (2024).
8. Loreau, M. In *Unsolved Problems in Ecology* (eds. Tilman, G. D., Dobson, A. & Holt, R. D.) 218–224 (Princeton University Press, 2020).
9. Wickman, J., Litchman, E. & Klausmeier, C. A. Eco-evolutionary emergence of macroecological scaling in plankton communities. *Science* **383**, 777–782 (2024).
10. Hatton, I. A., Dobson, A. P., Storch, D., Galbraith, E. D. & Loreau, M. Linking scaling laws across eukaryotes. *Proc. Natl. Acad. Sci. USA* **116**, 21616 (2019).
11. Kleiber, M. Body size and metabolism. *Hilgardia* **6**, 315–351 (1932).
12. Brown, J. H., Gillooly, J. F., Allen, A. P., Savage, V. M. & West, G. B. Toward a metabolic theory of ecology. *Ecology* **85**, 1771–1789 (2004).
13. Ghedini, G., Malerba, M. E. & Marshall, D. J. How to estimate community energy flux? A comparison of approaches reveals that size-abundance trade-offs alter the scaling of community energy flux. *Proc. R. Soc. Biol. Sci.* **287**, 20200995 (2020).
14. Antunes, A. C. et al. Environmental drivers of local abundance–mass scaling in soil animal communities. *Oikos* **2023**, e09735 (2023).
15. de Castro, F. & Gaedke, U. The metabolism of lake plankton does not support the metabolic theory of ecology. *Oikos* **117**, 1218–1226 (2008).
16. Cyr, H. & Pace, M. L. Allometric theory: Extrapolations from individuals to communities. *Ecology* **74**, 1234–1245 (1993).
17. DeLong, J. P., Hanley, T. C. & Vasseur, D. A. Competition and the density dependence of metabolic rates. *J. Anim. Ecol.* **83**, 51–58 (2014).
18. DeLong, J. P. & Hanson, D. T. Metabolic rate links density to demography in Tetrahymena pyriformis. *ISME J.* **3**, 1396–1401 (2009).
19. Ghedini, G., White, C. R. & Marshall, D. J. Does energy flux predict density-dependence? An empirical field test. *Ecology* **98**, 3116–3126 (2017).
20. Ghedini, G., Marshall, D. J. & Loreau, M. Phytoplankton diversity affects biomass and energy production differently during community development. *Funct. Ecol.* **36**, 446–457 (2022).
21. Malerba, M. E., White, C. R. & Marshall, D. J. Phytoplankton size-scaling of net-energy flux across light and biomass gradients. *Ecology* **98**, 3106–3115 (2017).
22. Nadler, L. E., Killen, S. S., McClure, E. C., Munday, P. L. & McCormick, M. I. Shoaling reduces metabolic rate in a gregarious coral reef fish species. *J. Exp. Biol.* **219**, 2802–2805 (2016).
23. Nørgaard, L. S., Ghedini, G., Phillips, B. L. & Hall, M. D. Energetic scaling across different host densities and its consequences for pathogen proliferation. *Funct. Ecol.* **35**, 475–484 (2021).
24. Malerba, M. E. & Marshall, D. J. Size-abundance rules? Evolution changes scaling relationships between size, metabolism and demography. *Ecol. Lett.* **22**, 1407–1416 (2019).
25. Field, C. B., Behrenfeld, M. J., Randerson, J. T. & Falkowski, P. Primary production of the biosphere: Integrating terrestrial and oceanic components. *Science* **281**, 237 (1998).
26. Hillebrand, H. et al. Cell size as driver and sentinel of phytoplankton community structure and functioning. *Funct. Ecol.* **36**, 276–293 (2022).
27. Finkel, Z. V. et al. Phytoplankton in a changing world: cell size and elemental stoichiometry. *J. Plankton Res.* **32**, 119–137 (2010).
28. Gjoni, V., Glazier, D. S., Wesner, J. S., Ibelings, B. W. & Thomas, M. K. Temperature, resources and predation interact to shape phytoplankton size–abundance relationships at a continental scale. *Glob. Ecol. Biogeogr.* **32**, 2006–2016 (2023).
29. Huete-Ortega, M., Cermeño, P., Calvo-Díaz, A. & Marañón, E. Isometric size-scaling of metabolic rate and the size abundance distribution of phytoplankton. *Proc. R. Soc. B Biol. Sci.* **279**, 1815–1823 (2011).
30. Marañón, E. Cell size as a key determinant of phytoplankton metabolism and community structure. *Annu. Rev. Mar. Sci.* **7**, 241–264 (2015).
31. Tatsumi, S. & Loreau, M. Partitioning the biodiversity effects on productivity into density and size components. *Ecol. Lett.* **26**, 1963–1973 (2023).
32. Glazier, D. S. Beyond the '3/4-power law': variation in the intra-and interspecific scaling of metabolic rate in animals. *Biol. Rev.* **80**, 611–662 (2005).
33. López-Sandoval, D. C., Rodríguez-Ramos, T., Cermeño, P., Sobrino, C. & Marañón, E. Photosynthesis and respiration in marine phytoplankton: Relationship with cell size, taxonomic affiliation, and growth phase. *J. Exp. Mar. Biol. Ecol.* **457**, 151–159 (2014).
34. Adler, P. B. et al. Competition and coexistence in plant communities: intraspecific competition is stronger than interspecific competition. *Ecol. Lett.* **21**, 1319–1329 (2018).
35. Long, Z. T. & Morin, P. J. Effects of organism size and community composition on ecosystem functioning. *Ecol. Lett.* **8**, 1271–1282 (2005).
36. Makarieva, A. M. et al. Mean mass-specific metabolic rates are strikingly similar across life's major domains: Evidence for life's metabolic optimum. *Proc. Natl. Acad. Sci. USA* **105**, 16994–16999 (2008).
37. Finkel, Z. V., Irwin, A. J. & Schofield, O. Resource limitation alters the ¾ size scaling of metabolic rates in phytoplankton. *Mar. Ecol. Prog. Ser.* **273**, 269–280 (2004).
38. Marañón, E., Cermeño, P., Rodríguez, J., Zubkov, M. V. & Harris, R. P. Scaling of phytoplankton photosynthesis and cell size in the ocean. *Limnol. Oceanogr.* **52**, 2190–2198 (2007).
39. An, J. H., Goo, E., Kim, H., Seo, Y.-S. & Hwang, I. Bacterial quorum sensing and metabolic slowing in a cooperative population. *Proc. Natl. Acad. Sci. USA* **111**, 14912–14917 (2014).
40. Janča, M. & Gvoždík, L. Costly neighbours: Heterospecific competitive interactions increase metabolic rates in dominant species. *Sci. Rep.* **7**, 5177 (2017).
41. Gallego, I., Venail, P. & Ibelings, B. W. Size differences predict niche and relative fitness differences between phytoplankton species but not their coexistence. *ISME J.* **13**, 1133–1143 (2019).
42. Litchman, E., Klausmeier, C. A., Schofield, O. M. & Falkowski, P. G. The role of functional traits and trade-offs in structuring phytoplankton communities: scaling from cellular to ecosystem level. *Ecol. Lett.* **10**, 1170–1181 (2007).
43. Papanikolopoulou, L. A. et al. Interplay between r- and K-strategists leads to phytoplankton underyielding under pulsed resource supply. *Oecologia* **186**, 755–764 (2018).
44. Karafas, S., Teng, S. T., Leaw, C. P. & Alves-de-Souza, C. An evaluation of the genus *Amphidinium* (Dinophyceae) combining evidence from morphology, phylogenetics, and toxin production, with the introduction of six novel species. *Harmful Algae* **68**, 128–151 (2017).
45. Glazier, D. S. Variable metabolic scaling breaks the law: from 'Newtonian' to 'Darwinian' approaches. *Proc. R. Soc. B Biol. Sci.* **289**, 20221605 (2022).
46. Chesson, P. Mechanisms of maintenance of species diversity. *Annu. Rev. Ecol. Syst.* **31**, 343–366 (2000).
47. Waters, J. S., Holbrook, C. T., Fewell, J. H. & Harrison, J. F. Allometric scaling of metabolism, growth, and activity in whole colonies of the seed-harvester ant pogonomyrmex californicus. *Am. Nat.* **176**, 501–510 (2010).
48. Padfield, D., Buckling, A., Warfield, R., Lowe, C. & Yvon-Durocher, G. Linking phytoplankton community metabolism to the individual size distribution. *Ecol. Lett.* **21**, 1152–1161 (2018).

49. Poulson-Ellestad, K. L. et al. Metabolomics and proteomics reveal impacts of chemically mediated competition on marine plankton. *Proc. Natl. Acad. Sci. USA* **111**, 9009 (2014).
50. Sjöberg, M., Albrectsen, B. & Hjältén, J. Truncated power laws: a tool for understanding aggregation patterns in animals? *Ecol. Lett.* **3**, 90–94 (2000).
51. Narla, A. V., Hwa, T. & Murugan, A. Dynamic coexistence driven by physiological transitions in microbial communities. Preprint at http://biorxiv.org/lookup/doi/10.1101/2024.01.10.575059 (2024).
52. Schindelin, J. et al. Fiji: an open-source platform for biological-image analysis. *Nat. Methods* **9**, 676–682 (2012).
53. Hillebrand, H., Dürselen, C.-D., Kirschtel, D., Pollingher, U. & Zohary, T. Biovolume calculation for pelagic and benthic microalgae. *J. Phycol.* **35**, 403–424 (1999).
54. White, C. R., Kearney, M. R., Matthews, P. G. D., Kooijman, S. A. L. M. & Marshall, D. J. A manipulative test of competing theories for metabolic scaling. *Am. Nat.* **178**, 746–754 (2011).
55. Williams, P. J., le, B. & Laurens, L. M. L. Microalgae as biodiesel & biomass feedstocks: Review & analysis of the bio-chemistry, energetics & economics. *Energy Environ. Sci.* **3**, 554–590 (2010).
56. Ghedini, G., Loreau, M. & Marshall, D. J. Community efficiency during succession: a test of MacArthur's minimisation principle in phytoplankton communities. *Ecology* **101**, e03015 (2020).

Acknowledgements

We are grateful to Michel Loreau, Jacopo Grilli, Onofrio Mazzarisi, and Isabel Gordo for their comments on an earlier version of this manuscript. We thank Moritz Klassen for help with data collection and the Imaging Facility of the Gulbenkian Institute for Molecular Medicine (GIMM, particularly José Marques) for assistance with image processing. This work was supported by a postdoctoral PONTE fellowship from the Fundação Calouste Gulbenkian-IGC to L.F. and a fellowship from "la Caixa" Foundation (LCF/BQ/PI21/11830001; ID 100010434) and the European Union's Horizon 2020 research and innovation programme under the Marie Sklodowska Curie grant agreement no. 847648 to G.G. G.G. is also supported by an ERC Starting Grant funded by the European Union (ERC, META_FUN, 101116029). Views and opinions expressed are however those of the author(s) only and do not necessarily reflect those of the European Union or the European Research Council. Neither the European Union nor the granting authority can be held responsible for them.

Author contributions

L.F. and G.G. conceived the idea for this manuscript. G.G. designed and performed the experiments. L.F. and G.G. analysed the data. G.G. drafted the manuscript and both authors contributed to the final version.

Competing interests

The authors declare no competing interests.

Additional information

Supplementary information The online version contains supplementary material available at https://doi.org/10.1038/s41467-024-54307-w.

Correspondence and requests for materials should be addressed to Lorenzo Fant or Giulia Ghedini.

Peer review information *Nature Communications* thanks Daniel Perkins and the other anonymous reviewers for their contribution to the peer review of this work. A peer review file is available.